Study of efficient semipolar (11-22) InGaN green micro-light-emitting diodes on highquality (11-22) GaN/sapphire template

Hongjian Li, Matthew S Wong, Michel Khoury, Bastien Bonef, Haojun Zhang, Yichao Chow, Panpan Li, Jared Kearns, Aidan A Taylor, Philippe de Mierry, et al.

▶ **To cite this version:**

Hongjian Li, Matthew S Wong, Michel Khoury, Bastien Bonef, Haojun Zhang, et al.. Study of efficient semipolar (11-22) InGaN green micro-light-emitting diodes on highquality (11-22) GaN/sapphire template. Optics Express, 2019, 10.1364/OE.27.024154 . hal-03023844

HAL Id: hal-03023844
https://hal.science/hal-03023844v1

Submitted on 25 Nov 2020

HAL is a multi-disciplinary open access archive for the deposit and dissemination of scientific research documents, whether they are published or not. The documents may come from teaching and research institutions in France or abroad, or from public or private research centers.

L'archive ouverte pluridisciplinaire **HAL**, est destinée au dépôt et à la diffusion de documents scientifiques de niveau recherche, publiés ou non, émanant des établissements d'enseignement et de recherche français ou étrangers, des laboratoires publics ou privés.

Research Article | Vol. 27, No. 17 | 19 Aug 2019 | OPTICS EXPRESS 24154
Optics EXPRESS

Study of efficient semipolar (11-22) InGaN green micro-light-emitting diodes on high-quality (11-22) GaN/sapphire template

HONGJIAN LI,[1,2,*] MATTHEW S. WONG,[1] MICHEL KHOURY,[1] BASTIEN BONEF,[1] HAOJUN ZHANG,[3] YICHAO CHOW,[1] PANPAN LI,[3] JARED KEARNS,[1] AIDAN A. TAYLOR,[1] PHILIPPE DE MIERRY,[4] ZAINURIAH HASSAN,[2] SHUJI NAKAMURA,[1,3] AND STEVEN P. DENBAARS[1,3]

[1]*Materials Department, University of California, Santa Barbara, CA 93106, USA*
[2]*Institute of Nano Optoelectronics Research and Technology, Universiti Sains Malaysia, 11800 USM, Penang, Malaysia*
[3]*Department of Electrical and Computer Engineering, University of California, Santa Barbara, CA 93106, USA*
[4]*CNRS-CRHEA, Rue Bernard Gregory, 06560 Valbonne, France*
**hongjianli@ucsb.edu.*

Abstract: We investigated the electrical and optical performances of semipolar (11-22) InGaN green μLEDs with a size ranging from 20 × 20 μm^2 to 100 × 100 μm^2, grown on a low defect density and large area (11-22) GaN template on patterned sapphire substrate. Atom probe tomography (APT) gave insights on quantum wells (QWs) thickness and indium composition and indicated that no indium clusters were observed in the QWs. The μLEDs showed a small wavelength blueshift of 5 nm, as the current density increased from 5 to 90 A/cm^2 and exhibited a size-independent EQE of 2% by sidewall passivation using atomic-layer deposition, followed by an extremely low leakage current of ~0.1 nA at −5 V. Moreover, optical polarization behavior with a polarization ratio of 40% was observed. This work demonstrated long-wavelength μLEDs fabricated on semipolar GaN grown on foreign substrate, which are applicable for a variety of display applications at a low cost.

© 2019 Optical Society of America under the terms of the OSA Open Access Publishing Agreement

1. Introduction

III-nitride based micro-light-emitting-diodes (μLEDs) are promising candidate for next-generation display applications, including near-eye displays and head-up displays. μLEDs offer advantages in high brightness, long operating lifespan, chemical robustness, and high luminous efficiency, compared to the current display technologies [1–3]. For high-resolution display applications that require ultra-small μLEDs, utilizing phosphor-free red, green and blue μLEDs is desired. Although high performance *c*-plane μLEDs have been developed and demonstrated [4–6], those LEDs experience a large blue-shift in wavelength with increasing current [7,8], which can be problematic for any display applications. The significant blue-shift in wavelength in conventional *c*-plane LEDs is due to the quantum confined Stark effect (QCSE), which corresponds to a high built-in electric fields in the *c*-plane direction [9–12]. One alternative approach is to employ LEDs grown on semipolar or nonpolar crystallographic orientations to alleviate or eliminate the influences of the QCSE. Semipolar LEDs also have several advantages such as low efficiency droop, high indium incorporation for long-wavelength emission and polarized light emission, which are beneficial for a variety of display applications [12–17]. Efficient semipolar LEDs on bulk GaN have been demonstrated, however, the use of semipolar bulk GaN substrates for μLED production remains impractical, since the substrates are too expensive and only commercially available in small area, while an enormous number of μLEDs is needed for display applications. On the

#367949 https://doi.org/10.1364/OE.27.024154
Journal © 2019 Received 20 May 2019; revised 19 Jul 2019; accepted 27 Jul 2019; published 8 Aug 2019

Optics EXPRESS

other hand, typical semipolar GaN materials grown on foreign substrates suffer from high density of basal stacking faults (BSFs) and other threading dislocations (TDs), which results in poor performance and low efficiency of the devices. Only a few groups have reported the efficient semipolar LEDs grown on foreign substrate. In our previous studies, we show that efficient long-wavelength semipolar (11-22) LEDs can be obtained by growing on low defect density and large area (11-22) GaN/sapphire template [18].

In this work, we investigated the electrical and optical properties of 520 nm semipolar (11-22) InGaN μLEDs with size ranging from 20 × 20 μm^2 to 100 × 100 μm^2, fabricated on low defect density and large area (11-22) GaN grown on sapphire substrate. To our knowledge, this is the first comprehensive study on the optical and electrical performances of efficient semipolar green μLEDs fabricated on foreign substrate. Structural characterization by atom probe tomography (APT) was carried out to investigate the grown materials microstructures.

2. Experimental

The LEDs were grown on a 2-inch (11-22) GaN/sapphire template by metal-organic chemical vapor deposition (MOCVD) at atmospheric pressure. Trimethylgallium (TMG), triethylgallium (TEG), trimethylindium (TMI), Trimethylaluminum (TMA), ammonia (NH_3), disilane (Si_2H_6), and magnesium (Cp_2Mg) were used as precursors and dopants. The growth and preparation details of the template have been reported elsewhere, which involved with a 3-step growth process on patterned r-plane sapphire substrates [18,19]. The semipolar (11-22) GaN/sapphire template was chemo-mechanically polished before the growth of the LEDs structure. Figure 1(a) is a 2 × 2 μm^2 atomic force microscopy (AFM) image of the semipoalr GaN/sapphire template, which shows a surface roughness of 0.1 nm. The X-ray diffraction (XRD) measurements (not presented here) show a full width at half maximum (FWHM) of 302 and 353 arcsec along [1-100] and [-1-123] direction, respectively, suggesting a high crystal quality of the semipolar (11-22) GaN/sapphire template. The final TDs density of the semipolar GaN/sapphire template is around 5 × 10^7 cm^{-2} with an BSFs density estimated to be around 0-70 cm^{-1}. The LEDs epitaxial structure consists of a 2.5-μm *n*-type GaN with Si concentration of 7 × 10^{18} cm^{-3}, a 150-nm $In_{0.03}Ga_{0.97}N$ strain-relaxed layer, 3 pairs InGaN/GaN multiple quantum wells (MQWs), a 15-nm *p*-type AlGaN electron-blocking layer (EBL), a 120-nm *p*-type GaN and a 15-nm *p* + GaN. The μLEDs were fabricated in squares with the edge length ranging from 20, 40, 60, 80, and 100 μm [4–6]. First, 110-nm indium-tin oxide (ITO) was deposited as a transparent and ohmic *p*-contact layer using electron-beam evaporation. The μLED mesas were defined using etching to the *n*-GaN layer using silicon tetrachloride in a reactive-ion etching (RIE) chamber. An omnidirectional reflector (ODR) consists of silicon dioxide and tantalum pentoxide, followed by aluminum oxide as the capping layer. 50-nm of silicon dioxide was blanket deposited by atomic-layer deposition (ALD) as a sidewall passivation layer, and buffered hydrofluoric acid was used to open a window for metal deposition [6]. A common metal contact consists of Al/Ni/Au (700/100/700 nm) was deposited using electron-beam evaporation. Finally, the μLEDs were diced, packaged onto silver headers, encapsulated using Dow Corning OE-6650 resin with a refractive index of 1.54, and measured in a calibrated integrating sphere.

Optics EXPRESS

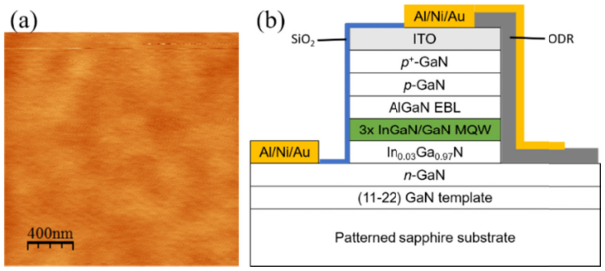

Fig. 1. (a) 2 × 2 μm^2 AFM image of the semipolar (11-22) GaN/sapphire template and (b) Schematic image of the epitaxial structure and μLEDs design.

3. Results and discussion

The composition, morphology and alloy distribution in the active region of the LEDs were investigated using APT. A FEI Helios 600 dual beam FIB instrument was used for the preparation of the needle shaped samples for the APT analysis [20]. APT experiments were performed with a Cameca 3000X HR Local Electrode Atom Probe (LEAP) operated in laser-pulse mode (13 ps pulse, 532 nm green laser, 10 μm laser spot size) with a sample-based temperature of 30 K. The laser pulse energy and the detection rate for the experiments were respectively set to 0.5 nJ and 0.005 atoms per pulse. The 3D reconstruction was carried out using a geometrical based algorithm implemented in the commercial software IVAS [21].

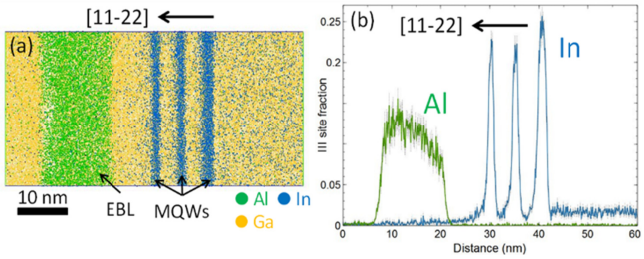

Fig. 2. (a) APT 3D volume extracted in the center of the global tip reconstruction showing the AlGaN EBL layer, the three InGaN/GaN MQWs and the top part of the InGaN buffer layer. (b) 1D concentration profile extracted from the APT reconstruction in (a) along the [11–22] direction. The sampling volume dimension is 30 × 30 × 60 nm^3 and the sampling step is 0.1 nm.

Figure 2(a) shows an APT 3D volume extracted in the center of the global tip reconstruction where the spatial resolution of the instrument in the depth direction is optimized. The active region can be clearly observed with defined InGaN/GaN QWs/quantum barriers (QBs) and AlGaN EBL. The InGaN buffer layer underneath the first InGaN QW can also be observed. In the reconstruction, the first grown InGaN QW appear to be wider than the two others. Also, In atoms are also visible in the GaN QBs. Figure 2(b) is a 1D concentration profiles extracted from the APT reconstruction in Fig. 1(a) and taken along the [11–22] direction. The Al, In and Ga III site fractions in the different layers can be directly measured from this profile. In Fig. 2(b), a concentration gradient in AlGaN EBL with a peak Al fraction of 0.13 can be observed along the depth direction since the TMA flow was ramping during the growth [18,22]. A 1D line profile of the image intensity in the growth direction (averaged over 17 lateral atomic columns) confirms that the first quantum well, 3.5 ± 0.2 nm, is thicker than wells two and three 2.6 ± 0.2 nm and 2.5 ± 0.2 nm. A possible reason for the thinner top two QWs is that these QWs grow under more lattice-matched conditions (biaxial stress) as compared to the first one [23]. Finally, as already noticed in Fig. 2(a), a fraction of In around 0.02 is measured in the QBs. A significant incorporation of In during the growth of the barrier layers is suspected and was already observed in our similar

Optics EXPRESS

growth on semipolar directions [22,24]. This can be likely better controlled with further epitaxial optimization and QB design.

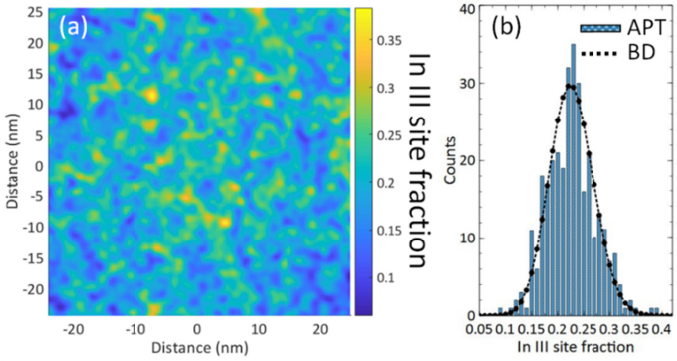

Fig. 3. (a) 2D In concentration map in the second QW and (b) Distribution of bin compositions of In and comparison with the binomial distribution for the case of random alloy.

Figure 3(a) is a 2D top view of the In distribution in the second InGaN well, where In rich and poor regions can be observed. The voxel size and delocalization parameters used to draw this 2D view are respectively 0.5 nm is X, Y, and Z and 1.5 nm [25,26]. No pattern of In segregation or clustering could be extracted from this 2D view. The corresponding statistical distribution analysis (SDA) for the In alloy fluctuation is shown in Fig. 3(b) [27]. The alloy distributions (blues bars) are compared to the binomial distribution (dotted line) as described in Ref [24]. SDAs were performed on the 3 InGaN QWs and the InGaN buffer layer. All investigated layers are random alloy and no clustering of In is observed.

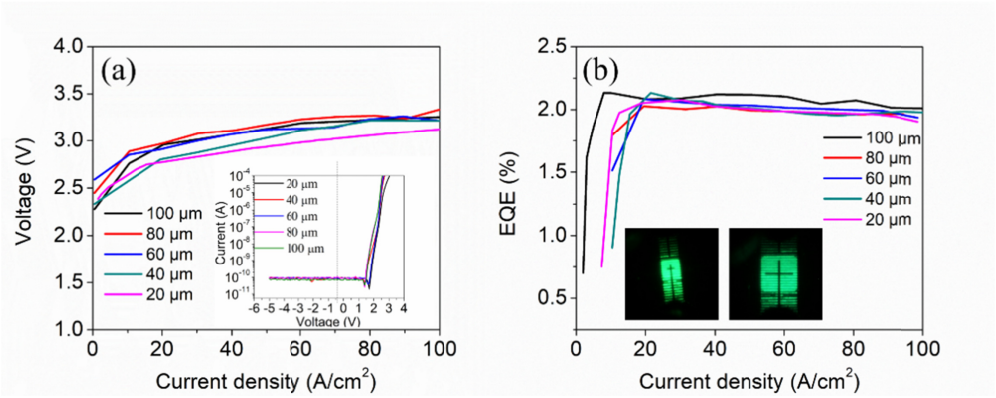

Fig. 4. (a) Forward current density-voltage characteristics of μLEDs with different sizes. The inset are the reverse characteristics. (b) EQE versus current density for different size μLEDs. The inset are the lumious image of 40 × 40 and 80 × 80 μm^2.

The current density-voltage characteristics of μLEDs are shown in Fig. 4(a). The μLEDs have consistent current density-voltage characteristics with turn-on voltage around 2.5 V and the forward voltages were ranged from 2.8 to 3.2 V at 60 A/cm^2 for the μLEDs size from 20 × 20 μm^2 to 100 × 100 μm^2. Also, the reverse characteristics for the different μLEDs sizes are presented in the inset figure. At a reverse voltage of −5 V, all the μLEDs with different sizes show an extremely low leakage current of ~0.1 nA, which is a strong evidence of low BSFs density in our semipolar (11-22) GaN/sapphire template as well as less sidewall damage of the fabricated devices. The inset figures in Fig. 4(b) show the lumious image of the 40 × 40 and 80 × 80 μm^2 devices. Very uniform electricial lumious image are observed even for the smaller size dimension devices, which is ascribed to the effective current spreading across

Optics EXPRESS

smaller mesa areas and the reduction of surface recombination and non-radiative recombination by sidewall passivation using ALD [6]. The EQEs versus current density of the different size μLEDs were plotted in Fig. 4(b). All the μLEDs demonstrated efficiency droop less than 10% until 100 A/cm^2, which has been observed in other semipolar GaN LEDs, and is a consequence of lowering the carrier density due to the large overlapping of wavefunctions in the QWs [11,12,16]. Moreover, the peak current density increases as the μLED dimensions shrinks, which is a key feature of μLEDs [2,4,6]. The shift in peak current density is attributed by the effects of non-radiative recombination, such as surface recombination, as the μLED size reduces. Finally, all μLEDs exhibited a size-independent EQE peak EQE about 2%, which behaved distinctly from what has been demonstrated in the literatures [2,4–6]. Typically, the peak EQE drops as the μLED dimensions shrinks due to non-radiative recombination generated from the sidewall damage and the surface recombination [33]. The size-independence in peak EQE in our μLEDs indicates that the μLED efficiency is constrained by other non-radiative recombination sites and is not limited by the sidewall damage and surface recombination. Although such EQE is still low as compared to the one grown on crystal perfect semipolar bulk GaN [15] or *c*-plane substrate [7,8], this is the best value demonstrated for semipolar green μLEDs grown on foreign substrate to date. We do believe that further improvements such as defect management of misfit dislocations (MDs) in the active region and other TDs would dramatically enhance the efficiency for those semipolar green μLEDs on sapphire substrate.

For the optical properties, Fig. 5(a) shows a comparison of electricial lumious blue-shift in wavelength between our semipolar (11-22) green μLED and typical *c*-plane green LEDs. The semipolar (11-22) green μLEDs exhibit very narrow wavelength blue-shift of 5 nm from 522 to 517 nm as the current density increases from 5 to 90 A/cm^2. Meanwhile, a large blue-shift of 16 nm from 536 to 520 nm with a significant shift at low current density for the *c*-plane green LEDs was observed. These results suggest that the piezoelectric field within the MQWs is dramatically reduced in the semipolar (11-22) μLEDs. Furthermore, the optical polarization property of the semipolar μLEDs was investigated. Semipolar and non-polar GaN LEDs on bulk GaN substrates have been reported with high polarization ratio due to their anisotropic polarized emission [28–31]. Polarization measurements were carried out under continuous-wave operation at room temperature. Details of the polarization setup can be found elsewhere [32]. The polarization ratio is defined as $\rho = (I_{[1\text{-}100]} - I_{[\text{-}1\text{-}123]})/(I_{[1\text{-}100]} + I_{[\text{-}1\text{-}123]})$, where I is the electroluminescent intensity [29]. From Fig. 5(b), the polarization ratio of our semipolar (11-22) μLEDs was about 40% and was independent on the current density. Such polarization ratio is similar to the blue-green LEDs reported on semipolar bulk GaN [28].

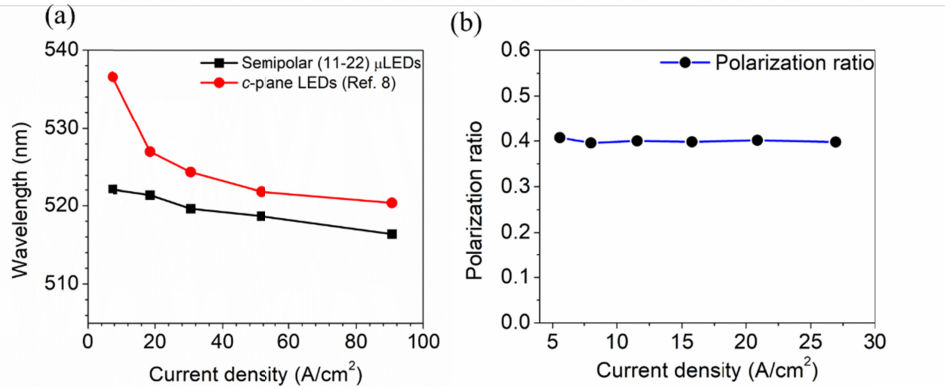

Fig. 5. (a) Blueshift in wavelength comparison between the semipolar (11-22) green μLEDs and c-plane green LED and (b) Polarization ratio of the semipolar (11-22) μLED with a size of 100 × 100 μm^2 at various current densities.

Optics EXPRESS

In conclusion, we demonstrate the semipolar (11-22) green μLEDs grown on low defect density semipolar (11-22) GaN/sapphire template. The μLEDs show a small blue-shift of 5 nm from 5 to 90 A/cm^2 and a high optical polarization ratio of 40%. Also, the μLEDs exhibit size-independent peak EQE of 2%. With further improvements in the materials quality, epitaxial structure and fabrication process, long-wavelength semipolar μLEDs fabricated on high quality, large area and low cost GaN/sapphire template is a promising candidate for μLED display applications due to the advantages such as size-independent EQE, extremely low leakage current, small wavelength blue-shift, low efficiency droop and high polarization ratio.

Funding

CREST Malaysia.

References

1. J. Day, J. Li, D. Y. C. Lie, C. Bradford, J. Y. Lin, and H. X. Jiang, "III-Nitride full-scale high-resolution microdisplays," Appl. Phys. Lett. **99**(3), 031116 (2011).
2. F. Olivier, S. Tirano, L. Dupré, B. Aventurier, C. Largeron, and F. Templier, "Influence of size-reduction on the performances of GaN-based micro-LEDs for display application," J. Lumin. **191**, 112–116 (2017).
3. V. W. Lee, N. Twu, and I. Kymissis, "Micro-LED Technologies and Applications frontline technology," Inf. Disp. **32**(6), 16–23 (2016).
4. D. Hwang, A. Mughal, C. D. Pynn, S. Nakamura, and S. P. DenBaars, "Sustained high external quantum efficiency in ultrasmall blue III-nitride micro-LEDs," Appl. Phys. Express **10**(3), 032101 (2017).
5. D. Hwang, A. J. Mughal, M. S. Wong, A. I. Alhassan, S. Nakamura, and S. P. DenBaars, "Micro-light-emitting diodes with III–nitride tunnel junction contacts grown by metalorganic chemical vapor deposition Sustained high external quantum efficiency in ultrasmall blue III–nitride micro-LEDs," Appl. Phys. Express **11**(1), 012102 (2018).
6. M. S. Wong, D. Hwang, A. I. Alhassan, C. Lee, R. Ley, S. Nakamura, and S. P. DenBaars, "High Efficiency of III-Nitride Micro-Light-Emitting Diodes by Sidewall Passivation Using Atomic Layer Deposition," Opt. Express **26**(16), 21324–21331 (2018).
7. A. I. Alhassan, N. G. Young, R. M. Farrell, C. Pynn, F. Wu, A. Y. Alyamani, S. Nakamura, S. P. DenBaars, and J. S. Speck, "Development of high performance green c-plane III-nitride light-emitting diodes," Opt. Express **26**(5), 5591–5601 (2018).
8. P. P. Li, Y. B. Zhao, H. J. Li, J. M. Che, Z. H. Zhang, Z. C. Li, Y. Y. Zhang, L. C. Wang, M. Liang, X. Y. Yi, and G. H. Wang, "Very high external quantum efficiency and wall-plug efficiency 527 nm InGaN green LEDs by MOCVD," Opt. Express **26**(25), 33108–33115 (2018).
9. D. F. Feezell, M. C. Schmidt, S. P. DenBaars, and S. Nakamura, "Development of Nonpolar and Semipolar InGaN/GaN Visible Light-Emitting Diodes," MRS Bull. **34**(5), 318–323 (2009).
10. H. Masui, S. Nakamura, S. P. DenBaars, and U. K. Mishra, "Nonpolar and semipolar III-nitride light-emitting diodes: Achievements and challenges," IEEE Trans. Electron Dev. **57**(1), 88–100 (2010).
11. D. F. Feezell, J. S. Speck, S. P. DenBaars, and S. Nakamura, "Semipolar (20-21) InGaN/GaN light-emitting diodes for high-efficiency solid-state lighting," IEEE/OSA. J. Disp. Technol. **9**(4), 190–198 (2013).
12. S. H. Oh, B. P. Yonkee, M. Cantore, R. M. Farrell, J. S. Speck, S. Nakamura, and S. P. DenBaars, "Semipolar III-nitride light-emitting diodes with negligible efficiency droop up to ~1 W," Appl. Phys. Express **9**(10), 102102 (2016).
13. D. L. Becerra, Y. Zhao, S. H. Oh, C. D. Pynn, K. Fujito, S. P. DenBaars, and S. Nakamura, "High-power low-droop violet semipolar (30-3-1) InGaN/GaN light-emitting diodes with thick active layer design," Appl. Phys. Lett. **105**(17), 171106 (2014).
14. Y. Zhao, Q. Yan, C. Y. Huang, S. C. Huang, P. S. Hsu, S. Tanaka, C. C. Pan, Y. Kawaguchi, K. Fujito, C. G. Van de Walle, and J. S. Speck, "Indium incorporation and emission properties of nonpolar and semipolar InGaN quantum wells," Appl. Phys. Lett. **100**(20), 201108 (2012).
15. S. Yamamoto, Y. Zhao, C. C. Pan, R. B. Chung, K. Fujito, J. Sonoda, S. P. DenBaars, and S. Nakamura, "High-efficiency single-quantum-well green and yellow-green light-emitting diodes on semipolar (20-21) GaN substrates," Appl. Phys. Express **3**(12), 122102 (2010).
16. Y. Zhao, S. Tanaka, C. C. Pan, K. Fujito, D. Feezell, J. S. Speck, S. P. DenBaars, and S. Nakamura, "High-power blue-violet semipolar (20-2-1) InGaN/GaN light-emitting diodes with low efficiency droop at 200 A/cm^2," Appl. Phys. Express **4**(8), 82104 (2011).
17. C. D. Pynn, S. J. Kowsz, S. H. Oh, H. Gardner, R. M. Farrell, S. Nakamura, J. S. Speck, and S. P. DenBaars, "Green semipolar III-nitride light-emitting diodes grown by limited area epitaxy," Appl. Phys. Lett. **109**(4), 041107 (2016).
18. H. Li, M. Khoury, B. Bonef, A. I. Alhassan, A. J. Mughal, E. Azimah, M. E. A. Samsudin, P. De Mierry, S. Nakamura, J. S. Speck, and S. P. DenBaars, "Efficient Semipolar (11-22) 550 nm Yellow/Green InGaN Light-Emitting Diodes on Low Defect Density (11-22) GaN/Sapphire Templates," ACS Appl. Mater. Interfaces **9**(41),

Optics EXPRESS

36417–36422 (2017).
19. F. Tendille, P. De Mierry, P. Vennéguès, S. Chenot, and M. Teisseire, "Defect reduction method in (11-22) semipolar GaN grown on patterned sapphire substrate by MOCVD: Toward heteroepitaxial semipolar GaN free of basal stacking faults," J. Cryst. Growth **404**(15), 177–183 (2014).
20. K. Thompson, D. Lawrence, D. J. Larson, J. D. Olson, T. F. Kelly, and B. Gorman, "In situ site-specific specimen preparation for atom probe tomography," Ultramicroscopy **107**(2-3), 131–139 (2007).
21. F. Vurpillot, B. Gault, B. P. Geiser, and D. J. Larson, "Reconstructing atom probe data: A review," Ultramicroscopy **132**, 19–30 (2013).
22. R. Shivaraman, Y. Kawaguchi, S. Tanaka, S. P. DenBaars, S. Nakamura, and J. S. Speck, "Comparative analysis of (20-21) and (20-2-1) semipolar GaN light emitting diodes using atom probe tomography," Appl. Phys. Lett. **102**(25), 251104 (2013).
23. P. de Mierry, L. Kappei, F. Tendille, P. Vennéguès, M. Leroux, and J. Zuniga-Perez, "Green emission from semipolar InGaN quantum wells grown on low-defect (11-22) GaN templates fabricated on patterned r-sapphire," Phys. Status Solidi, B Basic Res. **253**(1), 105–111 (2016).
24. M. Khoury, H. Li, B. Bonef, L. Y. Kuritzky, A. J. Mughal, S. Nakamura, J. S. Speck, and S. P. DenBaars, "Semipolar (20-21) GaN templates on sapphire: 432 nm InGaN light-emitting diodes and light extraction simulations," Appl. Phys. Express **11**(3), 036501 (2018).
25. B. Bonef, M. Catalano, C. Lund, S. P. Denbaars, S. Nakamura, U. K. Mishra, M. J. Kim, and S. Keller, "Indium segregation in N-polar InGaN quantum wells evidenced by energy dispersive X-ray spectroscopy and atom probe tomography," Appl. Phys. Lett. **110**(14), 143101 (2017).
26. K. L. Torres, M. Daniil, M. A. Willard, and G. B. Thompson, "The influence of voxel size on atom probe tomography data," Ultramicroscopy **111**(6), 464–468 (2011).
27. M. P. Moody, L. T. Stephenson, A. V. Ceguerra, and S. P. Ringer, "Quantitative binomial distribution analyses of nanoscale like-solute atom clustering and segregation in atom probe tomography data," Microsc. Res. Tech. **71**(7), 542–550 (2008).
28. Y. Zhao, S. Tanaka, Q. Yan, C. Y. Huang, R. B. Chung, C. C. Pan, K. Fujito, D. Feezell, C. G. Van de Walle, J. S. Speck, and S. P. DenBaars, "High optical polarization ratio from semipolar (20-2-1) blue-green InGaN/GaN light-emitting diodes," Appl. Phys. Lett. **99**(5), 51109 (2011).
29. N. Fellows, H. Sato, H. Masui, S. P. DenBaars, and S. Nakamura, "Increased polarization ratio on semipolar (11-22) InGaN/GaN light-emitting diodes with increasing indium composition," Jpn. J. Appl. Phys., **47**(10), 7854–7856 (2008).
30. A. Tyagi, Y. D. Lin, D. A. Cohen, M. Saito, K. Fujito, J. S. Speck, S. P. DenBaars, and S. Nakamura, "Stimulated Emission at Blue-Green (480 nm) and Green (514 nm) Wavelengths from Nonpolar (m-plane) and Semipolar (11-22) InGaN Multiple Quantum Well Laser Diode Structures," Appl. Phys. Express **1**(9), 091103 (2008).
31. S. E. Brinkley, Y.-D. Lin, A. Chakraborty, N. Pfaff, D. Cohen, J. S. Speck, S. Nakamura, and S. P. DenBaars, Polarized spontaneous emission from blue-green m-plane GaN-based light emitting diodes," Appl. Phys. Lett. **98**(1), 011110 (2011).
32. H. Masui, H. Yamada, K. Iso, H. Hirasawa, N. N. Fellows, J. S. Speck, S. Nakamura, and S. P. DenBaars, "Optical polarization of m-plane In-GaN/GaN light-emitting diodes characterized via confocal microscope," Phys. Status Solidi., A Appl. Mater. Sci. **205**(5), 1203–1206 (2008).
33. F. Olivier, A. Daami, C. Licitra, and F. Templier, "Shockley-Read-Hall and Auger non-radiative recombination in GaN based LEDs: A size effect study," Appl. Phys. Lett. **111**(2), 022104 (2017).

195.220.191.23 {ts '2019-09-11 02:55:35'}